DISTRIBUTION OF EMITTERS IN AN ELLIPTICAL SOURCE

E. Silver and W. Roney
Plasma Physics Laboratory, Princeton University
Princeton, New Jersey 08544

ABSTRACT

We present a simple technique for calculating emission profiles from elliptically shaped plasmas.

I. INTRODUCTION

Several plasma diagnostic experiments require Abel inversion techniques to determine the radial distribution of emitters from line integrated measurements. The detection of x-ray and microwave emission are two well-known examples which use this technique to deduce the radial profiles of electron temperature and density, respectively. Such calculations have been routinely performed for plasmas with circular cross sections using methods developed by Bockasten [1] and Barr [2]. Recently, there has been interest in inversion schemes that are applicable to non-circular plasma shapes. In particular, tokamaks possessing divertors, such as PDX and ASDEX (poloidal divertors), can produce plasmas with approximately elliptical cross sections.

Sauthoff and von Goeler [3] have discussed methods for reconstructing non-circular source distributions if the surfaces of constant emissivity are approximated by a series of poloidal harmonics. In this report we show that methods, normally applied to sources with circular symmetry, can be simply modified to yield the radial distribution for any elliptically shaped source.

II. CIRCULAR CASE REVISITED

We briefly review the Abel inversion procedure for surfaces with circular symmetry. Assuming surfaces of constant emissivity, $\varepsilon(r)$, with typical units of ergs/(cm^3 - sec), the total integrated intensity detected by an observer at vertical position $y = y_o$ (refer to Fig. 1) is

$$I(y = y_o) = \int_{-x_o}^{x_o} \varepsilon(r)\, dx \ \frac{\text{ergs}}{\text{cm}^2 - \text{sec}} \quad . \tag{1}$$

The circular symmetry allows this expression to be rewritten as

$$I(y) = 2\int_{y}^{r_o} \frac{\varepsilon(r)\ r dr}{\left(r^2 - y^2\right)^{1/2}} \quad . \tag{2}$$

for all lines of sight $y = y_o$. This integral is a form of Abel's equation and can readily be inverted; one particular result is

$$\varepsilon(r) = \frac{-1}{\pi r} \frac{d}{dr}\left[\int_{r}^{r_o} \frac{I(y)\ y dy}{\left(y^2 - r^2\right)^{1/2}}\right] \frac{\text{ergs}}{\text{cm}^3 - \text{sec}} \quad . \tag{3}$$

In practice, the I(y)'s are a set of intensities measured at discrete values of y. The continuous variation of the intensity between any two measured values, $I(y_n)$, $I(y_{n+1})$, $n = 0, 1, 2, 3\ldots$, for example, is approximated by a polynomial in y. The specific function used for each interval, Δy, between y_n and y_{n+1} is determined from a fit to the intensities $I(y_n)$ neighboring the interval.* The use of polynomials makes (3) readily integrable.

---

*Barr and Bockasten use an exact fit to 4 intensities.

III. ELLIPTICAL CASE

For the elliptical case, we seek a form similar to (2). Referring to Fig. 2, the elliptical surfaces, u, are also assumed to possess constant emissivity; these surfaces can be defined by

$$\frac{x^2}{a^2} + \frac{y^2}{b^2} = u^2, \quad 0 \le u^2 \le 1 \quad . \tag{4}$$

An observer viewing the plasma along the line of sight, ℓ, determined by the angular position, ξ, would detect an intensity I,

$$I(\xi) = \int_{x_1,y_1}^{x_2,y_2} \varepsilon(u)\, d\ell \quad . \tag{5}$$

Since $d\ell = dx\left(1 + dy^2/dx^2\right)^{1/2} = dx\left(1 + \tan^2 \xi\right)^{1/2} = dx/\cos \xi$, (5) becomes

$$I(\xi) = \int_{x_1}^{x_2} \varepsilon(u)\, \frac{dx}{\cos \xi} \quad . \tag{6}$$

To obtain the desired form of (2), the integral above must be written entirely in terms of the variable, u. Note that ξ, like y in (2), is constant for each measurement. The geometrical arrangement enables us to write

$$y = z - (P - x)\tan \xi \quad . \tag{7}$$

Using (4,7) to remove the x and implicit y dependence in (6), in favor of the constant, $\tan\varepsilon$, yields

$$I(\xi) = 2ab\int_{u_t}^{1} \frac{\varepsilon(u)\ u\,du}{\cos\xi\left[b^2 + a^2\tan^2\xi\right]^{1/2}\left[u^2 - \frac{(z - P\tan\xi)^2}{b^2 + a^2\tan^2\xi}\right]^{1/2}} \qquad (8)$$

where u_t is the surface tangent to the line of sight.

It can be shown that the line integral between (x_1,y_1) and (x_t,y_t) is equal to that from (x_t,y_t) to (x_2,y_2); therefore the factor of 2 is introduced. Note that if $a = b = r_o$ and $\xi = 0$, the expression above reduces to the integral for the circular case,

$$I(y = z) = 2r_o\int_{y/r_o}^{1} \frac{\varepsilon(u)\ u\,du}{\left(u^2 - \frac{y^2}{r_o^2}\right)^{1/2}} \quad \text{where } u = r/r_o \ . \qquad (9)$$

Further algebraic manipulation of (4,7) shows that the ratio

$$\frac{(z - P\tan\xi)}{\left(b^2 + a^2\tan^2\xi\right)^{1/2}} = u_t \ . \qquad (10)$$

Making the final substitution of variables,

$$\frac{a}{b}\tan\xi = \tan\phi$$

simplifies (8) which is written below:

$$I(\xi) = 2a\int_{u_t}^{1} \frac{\varepsilon(u)\ u\,du}{\frac{\cos\xi}{\cos\phi}\left(u^2 - u_t^2\right)^{1/2}} \ . \qquad (11)$$

It is important to note that the factor $\cos\xi/\cos\Phi$ depends only upon the line of sight and the ellipticity and is constant for each line integral. Equation (11) therefore has the same form as (2) and implies that the Abel inversion techniques of Bockasten or Barr may still be employed, but with one caveat. Rather than fitting the measured line intensities $I(\xi)$ at discrete ξ's to polynomials in u_t*, one instead fits the weighted line integrals $I(\xi)\cos\xi/\cos\Phi$. Equation (3) then becomes

$$\varepsilon(u) = \frac{-1}{\pi u}\frac{d}{du}\frac{1}{a}\int_u^1 \frac{J(u_t)\, u_t du_t}{\left(u_t^2 - u^2\right)^{1/2}} \quad , \tag{12}$$

where $J(u_t)$ is the polynomial in u_t that best describes the weighted measurement, $I(\xi)\cos\Phi/\cos\xi$. We conclude that any numerical method which uses (3) to evaluate the emissivity can be applied to arbitrary elliptical shapes by including the weighting factor.

As an example of this technique, we have simulated an experimental situation by numerically integrating the source function,

$$S(u) = \frac{1}{\sqrt{2\pi}\sigma}\, e^{\frac{-(u-0.4)^2}{2\sigma^2}} \quad \text{with } \sigma = 0.2 \quad , \tag{13}$$

along twenty chords of a plasma cross-section. Our results show that for a fixed set of $\left[(u_t)_i,\ i = 0, 1, 2...\right]$ our Abel inversion method is insensitive to the choice of lines of sight.

---

*$I(\xi) = I(u_t)$ due to the dependence of u_t on ξ (equation 10).

Tables 1 through 3 compare the Abel inverted emissivities, $\varepsilon(u)$, listed in column 6 with the analytical values, $S(u)$, listed in column 7 for three different plasma ellipticities. Figure 3 depicts a subset of the twenty chords listed in the tables while Figs. 4, 5, and 6 are plots of both the line integrals and associated inversions presented in the tables.

In summary, we have shown that any numerical method for calculating emission distributions from circular plasmas can easily be adopted for plasmas with arbitrary ellipticities.

ACKNOWLEDGMENTS

The authors wish to thank Dr. O. Okada for helpful discussions.

This work was supported by the United States Department of Energy Contract No. EY-76-C-02-3073.

REFERENCES

[1] K. Bockasten, Journal of the Optical Society of America, Vol. 51, No. 9, (1961).

[2] W. Barr, Journal of the Optical Society of America, Vol. 52, No. 8, (1962).

[3] N. R. Sauthoff and S. von Goeler, IEEE Transactions on Plasma Science, "Techniques for the Reconstruction of Two-Dimensional Images from Projections," Vol. PS-7, No. 3, (September, 1979); PPPL-1447, (1978).

TABLE 1

Ellipticity = 1.0, a = 40 cm, b = 40 cm

(1) u_t	(2) ξ	(3) ϕ	(4) LINE INTEGRAL	(5) WEIGHTED INTEGRAL	(6) INVERSION $\epsilon(u_t)$	(7) SOURCE $S(u_t)$
0.00	3.31	3.31	78.07	78.07	0.2970	0.2700
0.05	4.01	4.01	79.15	79.15	0.4323	0.4314
0.10	4.72	4.72	81.55	81.55	0.6470	0.6476
0.15	5.42	5.42	84.55	84.55	0.9131	0.9132
0.20	- 5.42	- 5.42	87.36	87.36	1.2104	1.2099
0.25	- 6.12	- 6.12	89.07	89.07	1.5068	1.5057
0.30	- 6.82	- 6.82	88.79	88.79	1.7618	1.7603
0.35	- 7.52	- 7.52	85.84	85.84	1.9348	1.9333
0.40	-14.17	-14.17	79.93	79.93	1.9958	1.9947
0.45	-14.87	-14.87	71.28	71.28	1.9339	1.9333
0.50	-15.57	-15.57	60.62	60.62	1.7602	1.7603
0.55	-16.28	-16.28	49.00	49.00	1.5052	1.5057
0.60	17.85	17.85	37.54	37.54	1.2092	1.2099
0.65	18.58	18.58	27.20	27.20	0.9127	0.9132
0.70	19.30	19.30	18.60	18.60	0.6472	0.6476
0.75	20.02	20.02	11.98	11.98	0.4314	0.4314
0.80	27.00	27.00	7.24	7.24	0.2702	0.2700
0.85	27.75	27.75	4.08	4.08	0.1591	0.1587
0.90	28.50	28.50	2.10	2.10	0.0837	0.0876
0.95	29.25	29.25	0.91	0.91	0.0618	0.0455

TABLE 2

Ellipticity = 0.75, a = 30 cm, b = 40 cm

(1) u_t	(2) ξ	(3) Φ	(4) LINE INTEGRAL	(5) WEIGHTED INTEGRAL	(6) INVERSION $\varepsilon(u_t)$	(7) SOURCE $S(u_t)$
0.00	3.31	2.49	58.60	58.55	0.2974	0.2700
0.05	4.01	3.01	59.43	59.36	0.4328	0.4316
0.10	4.72	3.54	61.26	61.17	0.6481	0.6483
0.15	5.42	4.07	63.55	63.43	0.9151	0.9149
0.20	- 5.42	- 4.07	65.66	65.53	1.2131	1.2122
0.25	- 6.12	- 4.60	66.98	66.81	1.5107	1.5092
0.30	- 6.82	- 5.12	66.78	66.57	1.7664	1.7644
0.35	- 7.52	- 5.65	64.54	64.29	1.9386	1.9365
0.41	-14.17	-10.72	60.14	59.34	1.9956	1.9940
0.46	-14.87	-11.26	53.24	52.47	1.9172	1.9163
0.51	-15.57	-11.81	44.80	44.08	1.7240	1.7237
0.56	-16.28	-12.35	35.66	35.05	1.4500	1.4502
0.61	17.85	13.58	26.63	26.08	1.1328	1.1329
0.66	18.58	14.15	18.75	18.33	0.8298	0.8296
0.72	19.30	14.72	12.36	12.06	0.5671	0.5664
0.77	20.02	15.29	7.60	7.41	0.3618	0.3603
0.84	27.00	20.91	3.68	3.51	0.1803	0.1799
0.89	27.75	21.53	1.82	1.73	0.1123	0.0951

TABLE 3

Ellipticity = 0.50, a = 20 cm, b = 40 cm

(1) u_t	(2) ξ	(3) ϕ	(4) LINE INTEGRAL	(5) WEIGHTED INTEGRAL	(6) INVERSION $\epsilon(u_t)$	(7) SOURCE $S(u_t)$
0.00	3.31	1.66	39.08	39.04	0.2971	0.2700
0.05	4.01	2.01	39.65	39.58	0.4326	0.4317
0.10	4.72	2.36	40.89	40.78	0.6483	0.6488
0.15	5.42	2.72	42.43	42.29	0.9160	0.9161
0.20	- 5.42	- 2.72	43.84	43.69	1.2145	1.2139
0.25	- 6.12	- 3.07	44.73	44.54	1.5129	1.5117
0.30	- 6.82	- 3.42	44.61	44.37	1.7690	1.7673
0.35	- 7.52	- 3.78	43.10	42.82	1.9406	1.9387
0.41	-14.17	- 7.19	40.17	39.26	1.9938	1.9926
0.46	-14.87	- 7.56	35.37	34.48	1.9029	1.9025
0.51	-15.57	- 7.93	29.51	28.70	1.6948	1.6952
0.57	-16.28	- 8.31	23.21	22.52	1.4069	1.4078
0.62	17.85	9.15	16.98	16.37	1.0743	1.0753
0.68	18.58	9.54	11.68	11.22	0.7678	0.7685
0.73	19.30	9.93	7.47	7.16	0.5086	1.5090
0.79	20.02	10.33	4.43	4.23	0.3119	0.3118
0.87	27.00	14.29	1.72	1.58	0.1257	0.1260
0.93	27.75	14.74	0.73	0.67	0.0650	0.0605

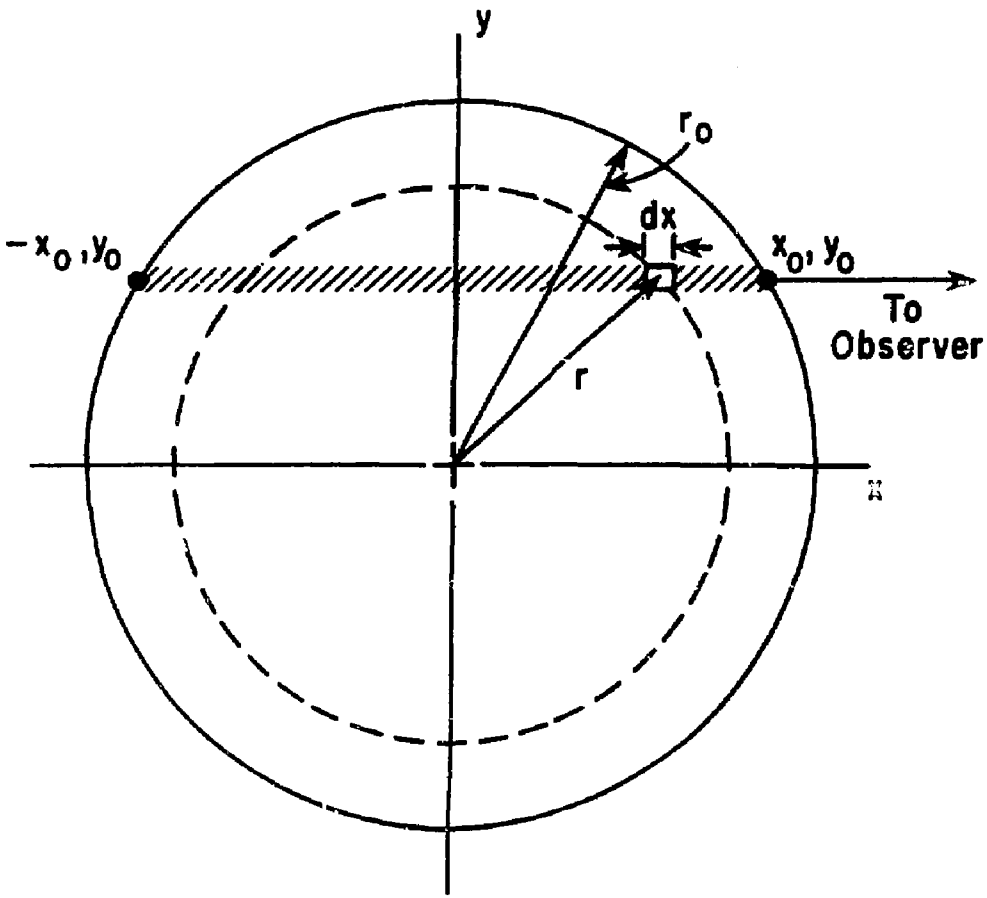

803021

Fig. 1. The geometrical relationship between the variables for a circular cross section.

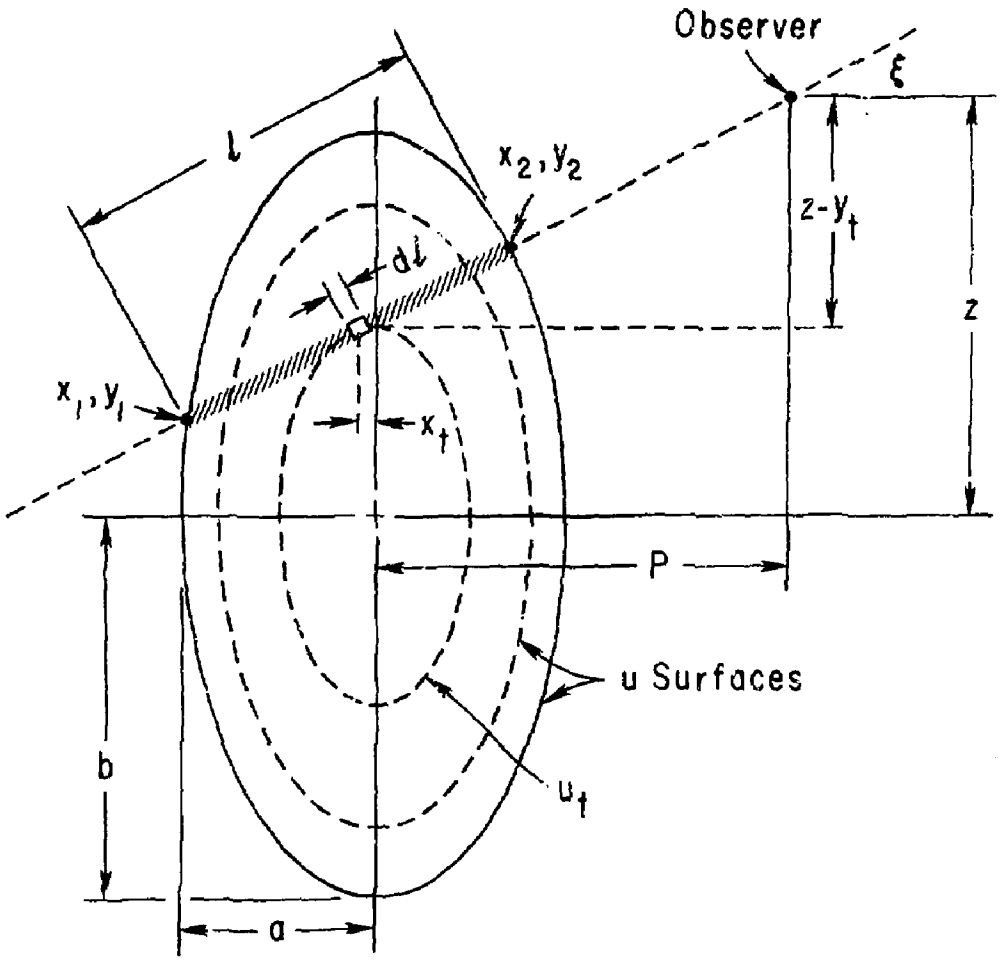

803040

Fig. 2. The geometrical relationship between the variables for an elliptical cross section.

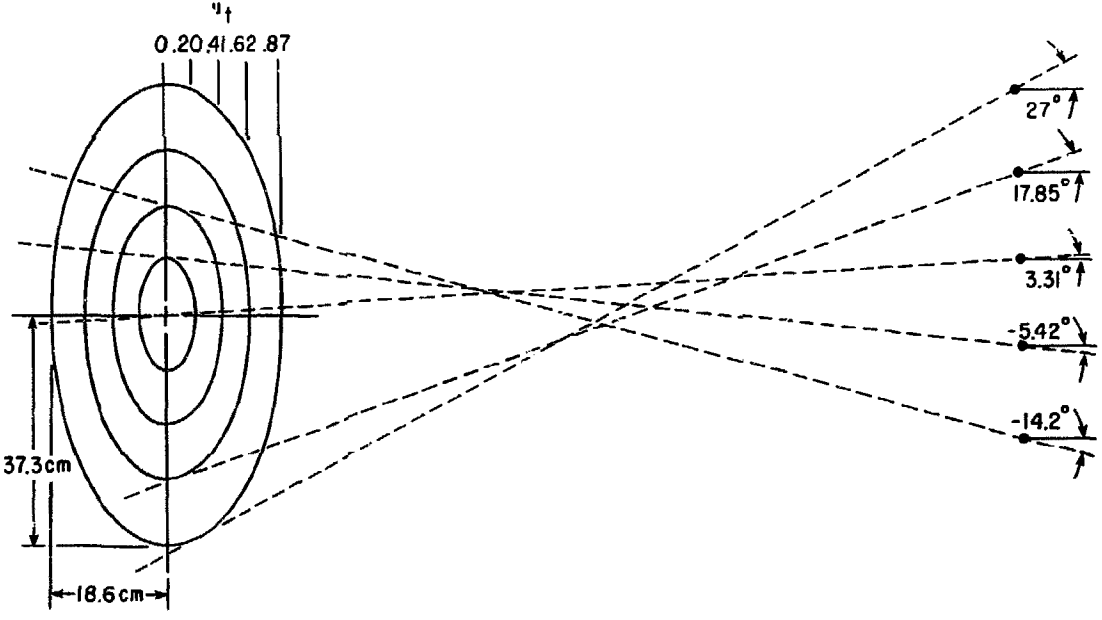

803019

Fig. 3. Five of the 20 lines of sight used to generate the line integrals plotted in Figs. 4-6.

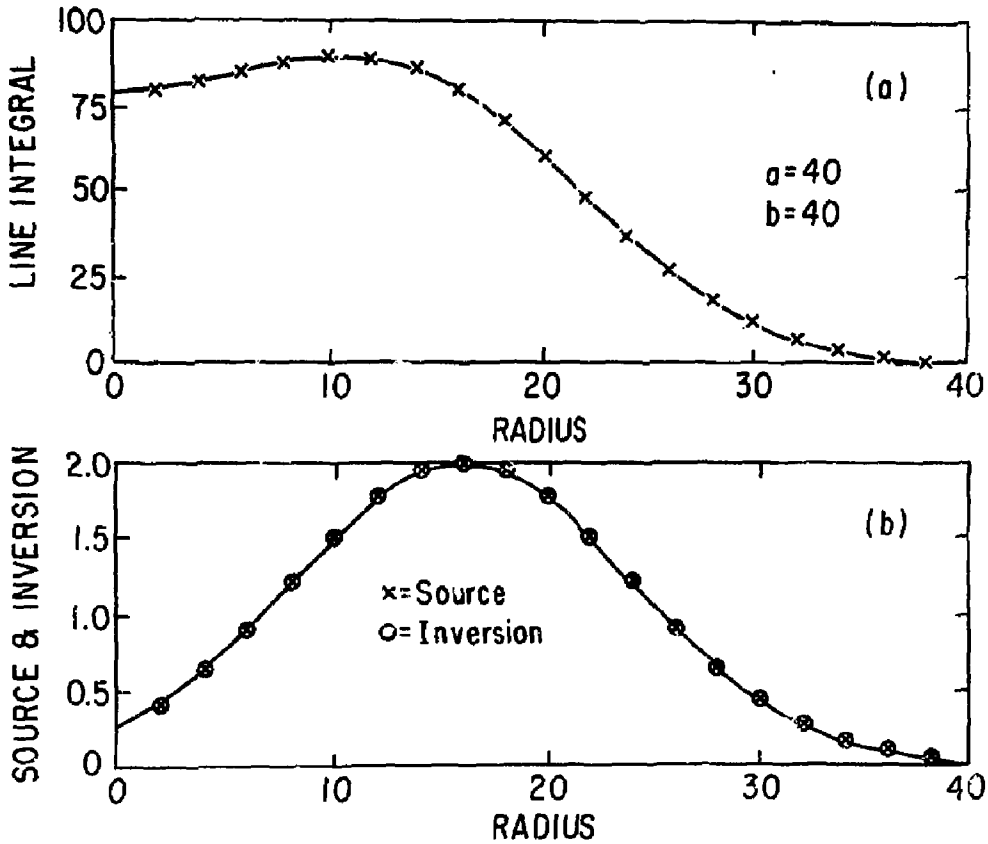

803022

Fig. 4. Plots of line integrals and their associated Abel inversions for ellipticity equal to 1 (a=40, b=40).

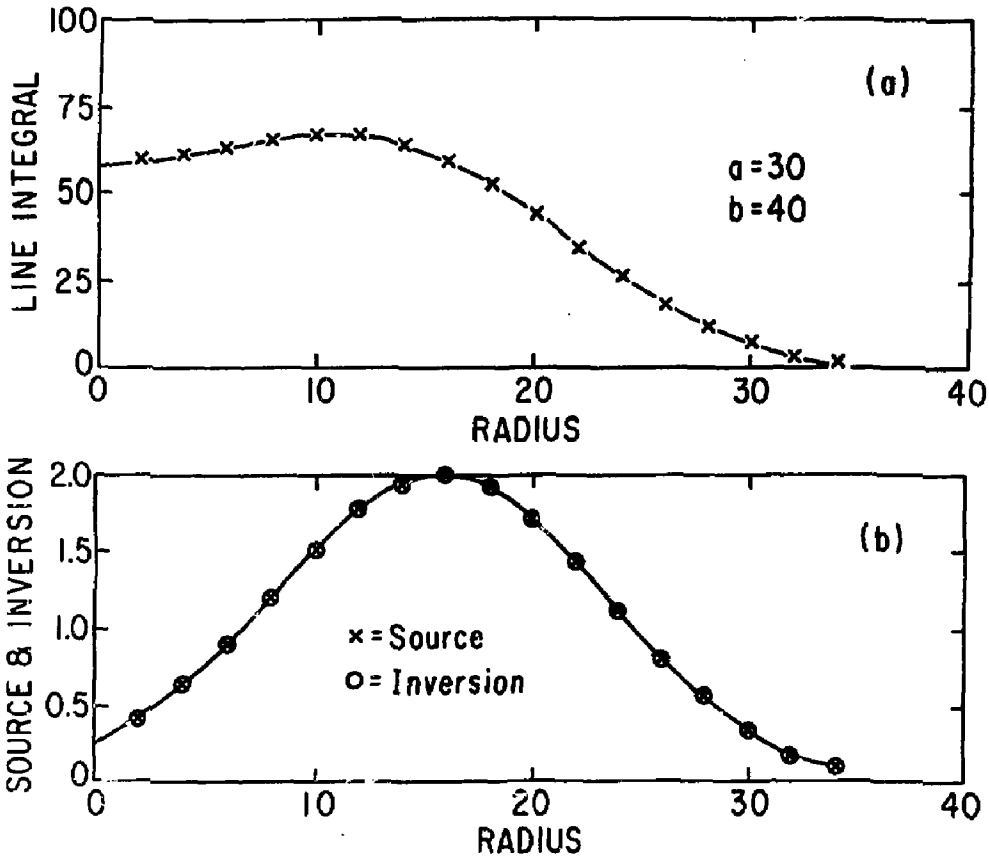

Fig. 5. Same as Fig. 4, but ellipticity = 0.75 (a=30, b=40).

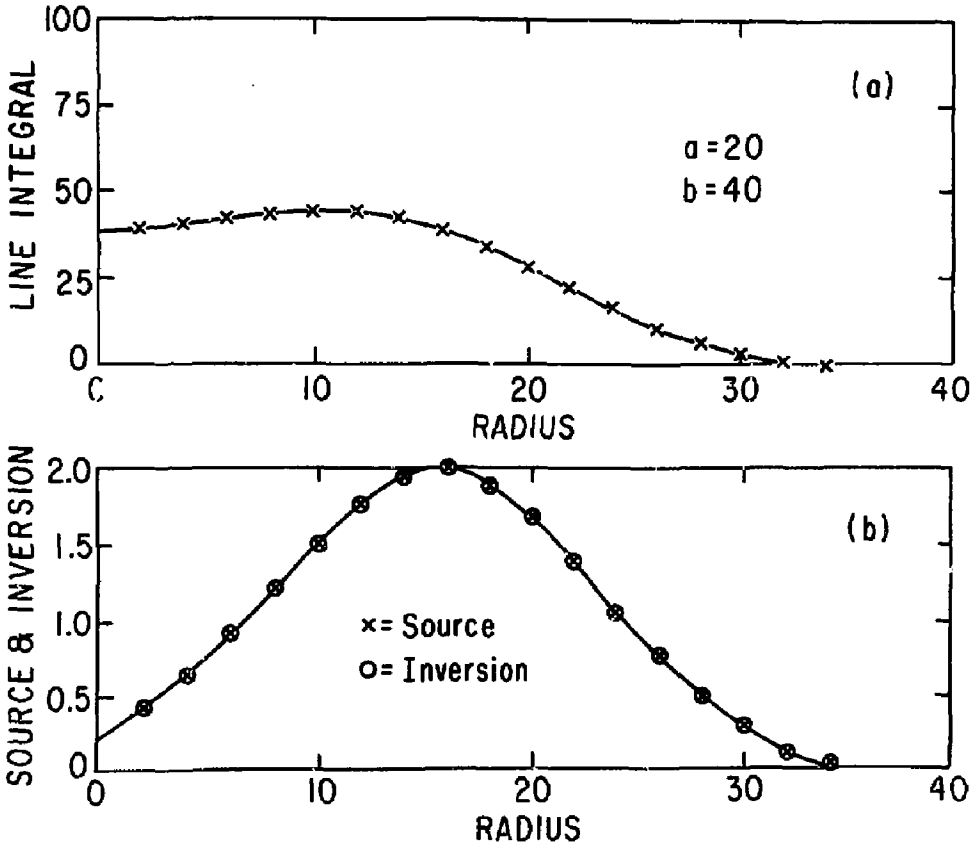

803023

Fig. 6. Same as Fig. 4, but ellipticity = 0.5 (a=20, b=40).